# 1P2-5

# Two-dimensional FDTD simulation of moving sources with arbitrary directivity

Takao Tsuchiya[1†] and Kei Inoue[1]
([1]Faculty of Sci. and Eng., Doshisha Univ.)

## 1. Introduction

As the speed of trains and airplanes increases, the noise prediction from moving vehicle is required. Some works have been reported that deal with moving omni-directional sources [1] or dipole sources [2]. However, it is necessary to consider more complex directivity for real sources. This paper focuses on point source cloud with arbitrary directivity. We theoretically derive the radiated sound in the two-dimensional field when a point source cloud moves and investigate its validity through numerical experiments using the 2-D finite difference-time domain (FDTD) method.

## 2. Theory

### 2.1 Moving monopole source

As shown in Fig. 1, we first consider the case where a monopole source is moving with a constant vcelocity $v_S$ in the *x*-direction. A 2-D fundamental solution is given as [3,4]

$$p_m \approx j\frac{Q}{4}\sqrt{\frac{2}{\pi kR}}\frac{e^{j(kR-\omega t)}}{\sqrt{1-M_S\cos\theta}} \quad (1)$$

where $Q$ is the source amplitude, $k=\omega/c_0$ is the wave number, $\omega$ is the angular frequency of the source, $M_S=v_S/c_0$ is the Mach number of the monopole.

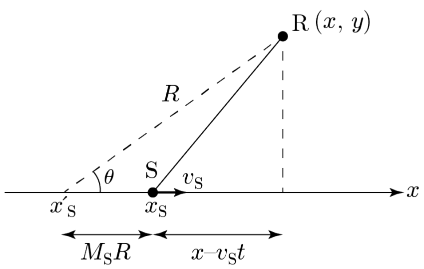


**Fig. 1** Positioning of a moving monopole source and a stationary receiver.

### 2.2 Moving point source cloud

We next consider a moving point source cloud as shown in Fig. 2 (a). Considering the *i*-th point source $S_i$ in the source cloud as shown in Fig. 2 (b), the distance $\tilde{r}_i$ to the receiver R is given for $\delta \ll R$ as [3]

$$\tilde{r}_i = \gamma^2\sqrt{(x-v_s-\delta x_i)^2+(y-\delta y_i)^2(1-M_s^2)}$$

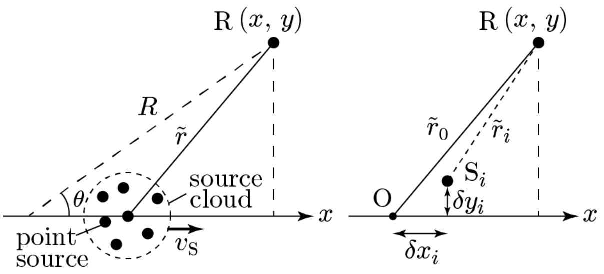


(a) point source cloud (b) *i*-th point source $S_i$

**Fig. 2** Moving point source cloud.

$$\approx \gamma^2 R(1-M_s\cos\theta)$$

$$\times\left(1-\frac{\delta x_i(\cos\theta-M_s)+\delta y_i(1-M_s^2)\sin\theta}{R(1-M_s\cos\theta)^2}\right) \quad (2)$$

where $\gamma=1/\sqrt{1-M_s^2}$ and $\delta x_i$ and $\delta y_i$ are distance from the center of cloud O. So, the sound pressure from the *i*-th point source is given as

$$p_i \approx j\frac{Q}{4}\sqrt{\frac{2}{\pi kR}}$$

$$\times\frac{1}{\sqrt{1-M_S\cos\theta}}e^{j\left(kR-\omega t-k\frac{\delta x_i\cos\theta+\delta y_i\sin\theta}{1-M_S\cos\theta}\right)} \quad (3)$$

So the sound pressure from the moving source cloud is given as

$$p \approx \sum_{i=1}^{N} p_i = j\frac{Q}{4}\sqrt{\frac{2}{\pi kR}}\frac{1}{\sqrt{1-M_S\cos\theta}}$$

$$\times\sum_{i=1}^{N} e^{j\left(kR-\omega t-k\frac{\delta x_i\cos\theta+\delta y_i\sin\theta}{1-M_S\cos\theta}\right)} \quad (4)$$

## 3. Numerical experiments

Numerical experiments were performed by the CE-FDTD (IWB) method [3-7]. Figure 3 (a) shows a 2-D numerical model for the directivity of point source cloud. The grid size is $\Delta$=8 mm, time step is $\Delta t$=23.29 $\mu$s, and sound speed is $c_0 = 340$ m/s, so

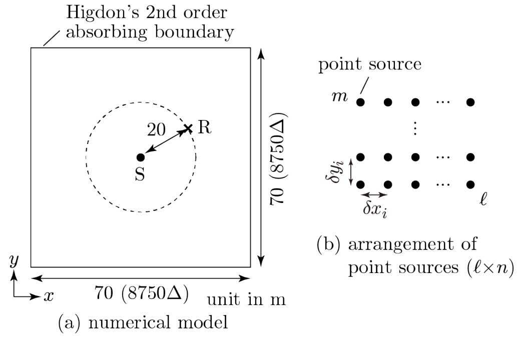


Fig. 3 Numerical model for point source cloud.

E-mail: †ttsuchiy@mail.doshisha.ac.jp

the Courant number $\chi$ is 0.99. The boundary condition is the Higdon's second order absorbing boundary. S is the center of the point source cloud and R is the receiver located on a circle with a radius of 10 m. A 20-cycles sinusoidal burst was emitted from the source. Figure 3 (b) shows the arrangement of point sources. The point sources are arranged in a $\ell \times m$ regular rectangular pattern, where $\ell$ and $m$ are the number of sound sources in $x$ and $y$ directions, respectively. All sound source spacings are set at 0.1 m.

Fig. 4 shows the directivity of stationary point source cloud for $\ell$=3, 6, 9 and $m$=3, 6, 9 with the source frequency of 500 Hz. In the figure, $X^{\ell}Y^{m}$ indicates the directivity for the $\ell \times m$ rectangular point source cloud. The calculation is performed with good accuracy even when the number of point sources is increased.

Figures 5 and 6 show the directivity of moving point source cloud for source velocities $M_S$ = 0.2 and 0.4, for $\ell$=3, 6, 9 and $m$=3, 6, 9 with the source frequency of 500 Hz. As the source speed is increased, the front-to-back ratio increases with the source velocity, and the beam width narrows. In particular, the effect of the movement is particularly pronounced when the main beam coincides with the moving direction of the source. Figure 7 shows the RMS error versus number of point sources $\ell$, $m$ for $M_S$ = 0, 0.2, 0.4 at source frequency of 500 Hz. The error increases with the number of sources and Mach number. If the $\ell$, $m$ are 5 or less, the error is almost within 1%, and the directivity is well realized.

These results indicate that this method is effective for the analysis of moving point source cloud with arbitrary directivity.

## References


1) H. Nakajima et al, J. Acoust. Soc. Jpn. **60**, 717 (2004). [in Japanese].
2) Y. Makino et al, Proc. Inter-Noise 2022 (2022).
3) T. Tsuchiya, Acoust. Sci. & Tech. **43**, 57 (2022).
4) T. Tsuchiya et al., J. Appl. Phys. **62**, SJ1015 (2023).
5) T. Tsuchiya, Jpn. J. Appl. Phys. **63**, 03SP23 (2024).
6) K. Kowalczyk et al, IEEE Trans. Audio Speech Lang. Process. **18**, 78 (2010).
7) T. Ishii et al., Jpn. J. Appl. Phys. **52**, 07HC11 (2013).


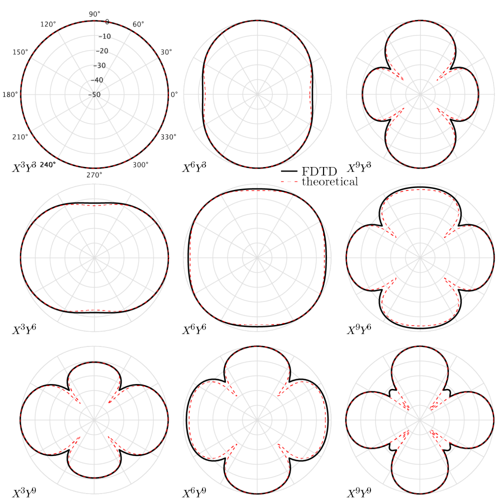


Fig. 4 Directivity of stationary point source cloud (500 Hz, $M_s = 0$).

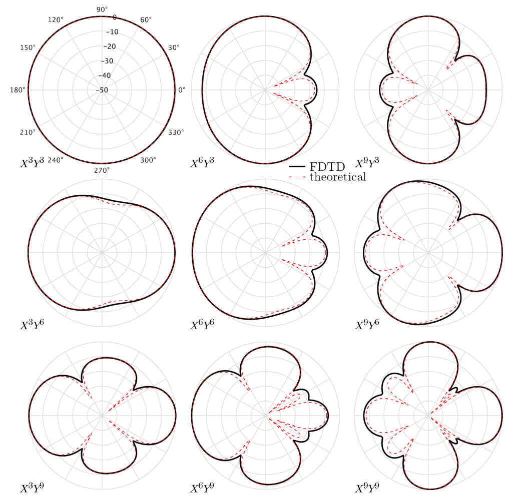


Fig. 5 Directivity of moving point source cloud (500 Hz, $M_s = 0.2$).

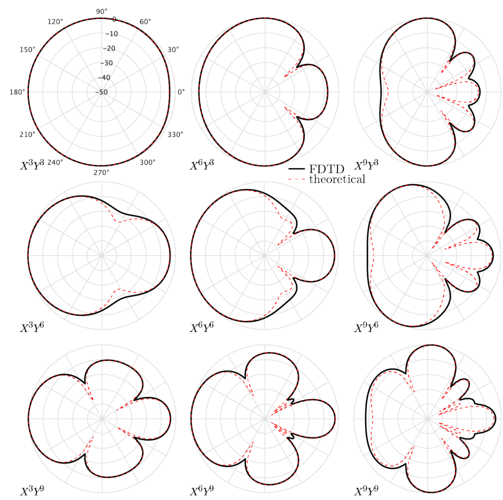


Fig. 6 Directivity of moving point source cloud (500 Hz, $M_s = 0.4$).

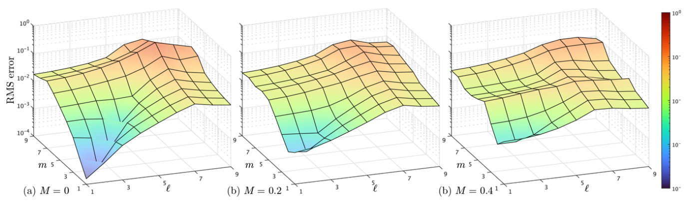


Fig. 7 RMS error against number of point sources ($\ell$, $m$) at frequency of 500 Hz.